Eco-friendly cost-effective approach for synthesis of ZnO nanoparticles and loaded on worn tire powdered activated carbon as a novel adsorbent to remove organic dyes from aqueous solutions: equilibrium, kinetic, regeneration and thermodynamic study

Shirin Afshin[a], Yousef Poureshgh[a], Yousef Rashtbari[a], Mehdi Fazlzadeh[b], Farshad Bahrami Asl[c], Asghar Hamzezadeh[a,*], Seyedeh Mahtab Pormazar[d,f,*]

[a]*Department of Environmental Health Engineering, School of Health, Ardabil University of Medical Sciences, Ardabil, Iran, Tel. +98 9143540015; emails: a.hamzezade@yahoo.com (A. Hamzezadeh), Tel. +98 9014515339; email: shirinafshin1990@gmail.com (S. Afshin), Tel. +989148092356; email: yusef.poureshg@gmail.com (Y. Poureshgh), Tel. +989383162079; email: u3f.rashtbari@gmail.com (Y. Rashtbari)*
[b]*Social Determinants of Health Research Center, Ardabil University of Medical Sciences, Ardabil, Iran, email: m.fazlzadeh@gmail.com*
[c]*Department of Environmental Health Engineering, School of Health, Urmia University of Medical Sciences, Urmia, Iran*
[d]*Environmental Science and Technology Research Center, Department of Environmental Health Engineering, School of Public Health, Shahid Sadoughi University of Medical Sciences, Yazd, Iran, Tel. +989139672497; email: smp.mahtab@gmail.com*
[f]*Student Research Committee, Shahid Sadoughi University of Medical Sciences, Yazd, Iran*

Received 11 June 2020; Accepted 1 April 2021

ABSTRACT

In the present research, activated carbon (AC) was prepared from worn tire specimens and was coated with zinc oxide nanoparticles (ZnO) obtained from pomegranate peel extract. The prepared adsorbent (AC-ZnO) was characterized by field-emission scanning electron microscopy, Brunauer–Emmett–Teller, X-ray diffraction and Fourier-transform infrared spectroscopy analyses. The performance of the AC-ZnO was investigated to remove Acid Black 1 (AB1) dye from aqueous solutions. The results of the adsorption experiment indicated that the removal efficiency declined with increasing dye concentration and solution pH but a decrease in adsorbent dosage caused the efficiency to decline. The findings suggest that the adsorption of AB1 onto the AC-ZnO obeyed the pseudo-second-order model. Equilibrium data were analyzed using the Langmuir and Freundlich isotherm. The data were best described by the Freundlich isotherm model and the maximum adsorption capacity of the AC-ZnO was 93.46 mg/g. Based on the thermodynamic parameters, the adsorption process was non-spontaneous at all temperatures and also the process was endothermic. The AC-ZnO could be regenerated and reused for several cycles and also has high efficiency (71.21%) in removing AB1 dye in the actual wastewater sample. It was implied that AC-ZnO could be employed effectively as a cheap and environmentally friendly adsorbent for AB1 dye removal from wastewater-containing dyes.

Keywords: Green synthesis; Activated carbon; Zinc oxide nanoparticles; Acid Black 1; Adsorption

* Corresponding authors.

1. Introduction

The discharge of dyes from textile industries into water resources has led to a significant increase in environmental pollution [1]. Over 100,000 different types of dyes are produced annually with a production rate of 7×10^5 tons/y, which about 36,000 tons/y are used by textile industries [2]. Among these, azo dyes are the largest and the most important group of synthetic dyes, as they are accounting for more than half of the synthetic dyes produced each year [3]. These organic dyes bearing the functional group (–N=N), which is a carcinogen, toxic and non-biodegradable in nature [4]. Dyes are responsible for water-borne diseases exhibiting symptoms such as hemorrhage, nausea, dermatitis, ulceration of the skin and mucous membranes, kidney damage, and a loss of bone marrow leading to anemia. Therefore, dyes must be removed from wastewaters to eliminate health hazards and prevent the destruction of the ecosystem [5]. In the last few decades, removing dyes from textile wastewaters has become a major challenge. Several treatment technologies such as coagulation and flocculation [6], electro-coagulation [7], electro-Fenton [8], chemical oxidation [9,10], membrane [11] and adsorption [12] have been employed to treat textile wastewaters. The adsorption process has been introduced as one of the best methods due to its simplicity, low cost, large availability and high efficiency [13–15]. From different types of materials used as adsorbents, activated carbon (AC) has been widely applied for the removal of dye from aqueous environments because of their unique characteristics [16]. Although AC is an effective adsorbent, its production from coal is very expensive and has low degradability [17]. Hence, researchers have focused on the production of AC from low-cost materials, with high carbon content and low inorganics [18]. Agricultural by-products such as rice husk [19], almond shell [20], palm shell [21], and peel or seeds of pomegranate [22] are used as raw material to synthesize porous carbon materials [23].

In addition, some waste materials could be recycled as precursors to generate AC [24]. Waste scrap tires are a big part of the world's waste in the modern life which is posing an environmental threat [25]. About 32% of the tires are carbon black in which the carbon content is nearly 70–75 wt.%. This carbon black is rather similar to AC and only carbon black has much less internal surface area [26]. Various studies have demonstrated the use of scrap tires as an AC sorbent for the removal of organic and inorganic pollutants from aqueous environments [27].

The application of nano-structure materials such as copper(II) oxide (CuO), iron oxide (FeO, Fe_2O_3 or Fe_3O_4) and zinc oxide (ZnO) nanoparticles as a powerful, non-toxic and green adsorbent is considered to impregnated on the surface of AC [28]. There are several advantages of nanoparticles utilization such as a huge number of active sites and selectivity properties; more importantly, when they are utilized as an adsorbent, their separation from aqueous solution is not difficult [25]. Amongst various nanoparticles, ZnO has been attracting great attention because of its dye adsorption properties. It benefits from having very spacious pores and easily available [29]. Since ZnO contains about 80% zinc, it has high adsorption capacity and well predictable reaction kinetics [29]. Various chemical methods have been proposed for the synthesis of ZnO NPs, such as the reaction of zinc with alcohol, vapor transport, hydrothermal synthesis, precipitation method, etc. However, these methods suffer various disadvantages due to the involvement of high temperature and pressure conditions and the use of toxic chemicals. Green synthesis approaches are gaining interest circumventing the high costs and usage of toxic chemicals and harsh conditions for reduction and stabilization [30]. Recently, plant extracts including *Peganum harmala* seed [31], flower [32], *Cassia fistula* plant [33], *Hibiscus sabdariffa* leaf [34], *Moringa oleifera* leaf [35], and so forth have been used to synthesize ZnO and other nanoparticles.

In the present study, the extract of pomegranate peel was utilized as a stabilizing agent for the preparation of the ZnO nanoparticles (ZnO NPs). Then, the ZnO NPs were coated on the AC derived from the worn tire specimens. According to the literature review, no studies on the uptake of Acid Black 1 (AB1) dye by the AC-ZnO have been conducted to date. Hence, in this study, the efficiency of the AC-ZnO in AB1 dye removal at different operational parameters was investigated.

2. Materials and methods

2.1. Materials

AB1 was obtained from Alvan Sabet Co., Hamadan, Iran. The properties of the dye have been shown in Table 1 [36]. 0.1 M NaOH, and HCl, used to adjust solution pH and zinc chloride ($ZnCl_2$), used to synthesize the adsorbent, were purchased from Merck & Co., Germany.
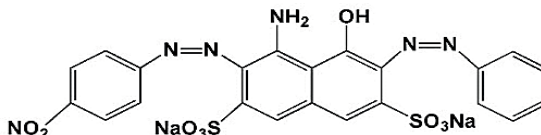
2.2. Activated carbon preparation

The worn tire specimens were first crushed to 0.5–2 cm. Next, they were immersed in concentrated phosphoric acid at room temperature for 48 h for activation. Then, they were poured into a cylindrical steel reactor. To accomplishment pyrolysis, the reactor was transferred to an electric furnace (HL40P) at a temperature of 500°C and a speed of 5°C/min for 2 h. Afterwards, the product of this step was sonicated by an ultrasonic device with a frequency of 37 kHz to generate powdered activated carbon and to create more pores. The obtained powder was then washed 4–6 times with deionized water to reach pH 7, and placed in an oven at 110°C for 2 h to dry completely. The resulting activated carbon was finally stored in a closed container away from moisture for future use [37].

2.3. Production of the zinc oxide nanoparticles by a green synthesis method

The pomegranate peel extract was used to synthesize the nanoparticles in a greenway. To end this, 30 g of the pomegranate peel was added to 500 mL of distilled water and mixed by a magnetic stirrer at 300 rpm at 80°C for 1 h. The extract was obtained and then cooled to ambient temperature. The solution was filtered using a 0.45 μm filter. The extract was mixed with zinc chloride (1 M) in a ratio of 2:3. The nanoparticle synthesis was detectable by the formation of white clusters. The synthesized nanoparticles

Table 1
Characteristics of AB1 dye

Dye symbol	AB1
Chemical structure	
Chemical formula	$Na_2C_{22}H_{14}N_6O_9S_2$
Molecular mass (g mol^{-1})	616.49
λ_{max} (nm)	618

were dried at ambient temperature for 1–2 d. In order to eliminate the interference from organic matter in the experiments, the nanoparticles were placed in an electric oven at 400°C for 2 h. Finally, the resulting product was stored for future use [31].

2.4. Loading of ZnO nanoparticles on activated carbon (AC-ZnO)

After the production of the AC and the synthesis of the zinc oxide nanoparticles, 0.05 g of the zinc nanoparticles was poured into 200 mL of distilled water and placed on a magnetic stirrer for 10 min to make the solution uniform. Then, 5 g of the AC was poured into the solution and placed on a magnetic stirrer at 500 rpm for 2 h to load the nanoparticles onto the AC. The modified AC was separated from the solution by means of a filter paper and then washed with double distilled water several times. The result production was placed in an oven at 95°C for 10 h to dry completely [38].

2.5. Characterization of adsorbent

The surface morphology of the non-modified and modified adsorbents was investigated with field emission scanning electron microscopy (FE-SEM). Fourier-transform infrared spectroscopy (FTIR) was utilized to characterize the surface functional groups of the AC and AC-ZnO using BRUKER Tensor 27 model FTIR spectrometer. X-ray diffraction (XRD) was employed to assess the phase structure of the samples by a Philips PAN-Analytical Diffractometer (Netherlands) equipped with a Cu Kα X-ray source. Brunauer–Emmett–Teller (BET) surface area was assessed by measuring the nitrogen adsorption–desorption isotherms at 77 K using Quantachrome (USA). The surface area, pore size and pore volume were evaluated using the t-plot method.

2.6. Batch adsorption study

So as to perform the batch adsorption experiments, 100 mL of the synthetic wastewater containing different concentrations of the dye (25–150 mg/L) was poured into a 100 mL Erlenmeyer glass flask. A certain dose of the adsorbent (0.25–2 g/L) was added to the solution and the solution pH was adjusted in the range of 3 to 11 using 0.1 M NaOH and 0.1 M HCl solution. The mixture was stirred at the rapid speed of 200 rpm at predetermined time intervals (2–90 min). After the adsorption process, the samples were filtered by using a 0.45-μm membrane filter. The residual concentration of AB1 dye was determined using a UV-vis spectrophotometer (HACH DR5000, USA) at the maximum wavelength of 618 nm [36]. The removal percentage of the dye by the AC-ZnO was calculated according to the following equation [39]:

$$R\left(\%\right) = \frac{C_0 - C}{C_0} \times 100 \tag{1}$$

where R (%) is dye removal efficiency, C_0 (mg/L) is the initial dye concentration (mg/L) and C is dye concentrations at time t (min).

The adsorption capacity of the AC-ZnO adsorbent to uptake AB1 Dye at the equilibrium was determined by the following equation:

$$q_e\left(mg/g\right) = \frac{C_0 - C_e}{m} V \tag{2}$$

where q_e (mg/g) is adsorption capacity, C_0 (mg/L) is the initial dye concentration, C_e (mg/L) is the equilibrium concentration of the dye in solution, V (L) is the volume of the aqueous solution and m (g) is the mass of the adsorbent.

2.7. Point of zero charge

The point of zero charge (pH$_{pzc}$) was used to quantify the net charge of the adsorbent (positive or negative). For this purpose, the initial pH values were adjusted in the range from 2 to 12 by adding 0.1 M HCl or 0.1 M NaOH. Then, 0.05 g of the adsorbent was added to several 100 mL Erlenmeyer flasks. The suspensions were shaken for 24 h until the equilibrium was achieved. Finally, the pH of the supernatant was measured, and the final pH values were plotted against the initial pH. The pH$_{pzc}$ is the point of intersection of the resulting curve, where initial pH = final pH [40].

3. Results and discussion

3.1. Characterization of the synthesized adsorbent

The shape and surface morphology of the non-modified and modified AC were investigated by a FE-SEM. Fig. 1
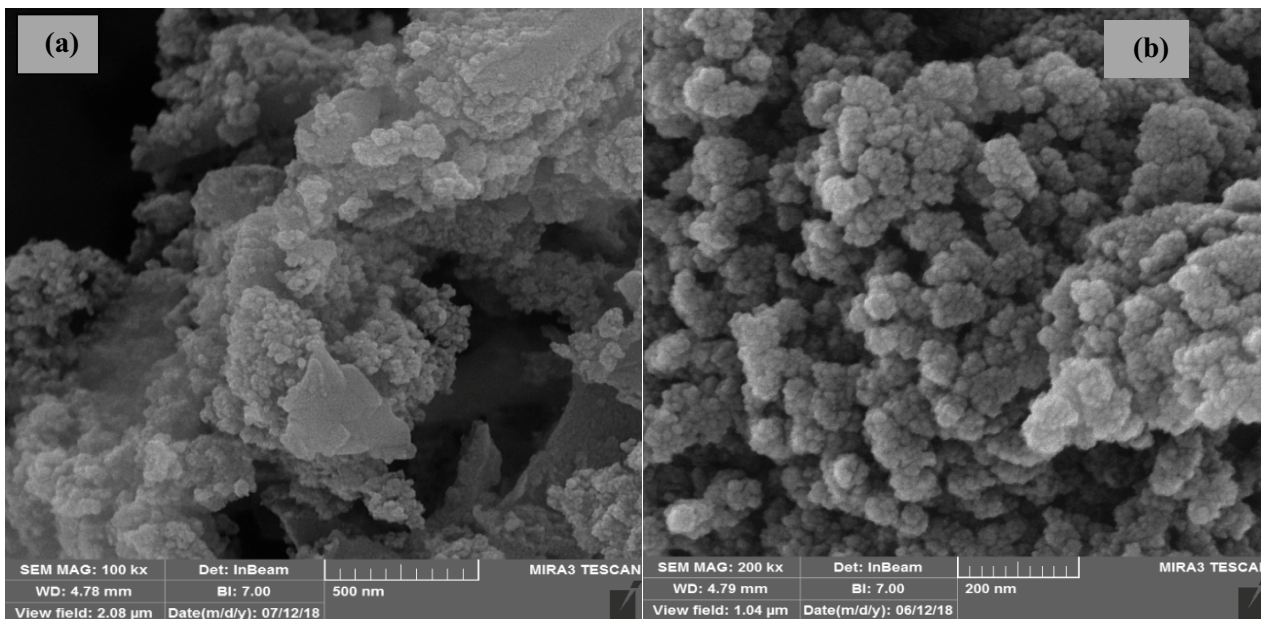
Fig. 1. FE-SEM images of the AC (a) and AC-ZnO nanoparticles (b).

shows the FE-SEM images of the AC and AC-ZnO. It seems that the ZnO nanoparticles have occupied the unevenness of the surface of the AC. As can be seen, the ZnO nanoparticles were relatively homogeneous and uniform on the adsorbent surface. In fact, the FE-SEM image illustrates that the filled pores of the AC were occupied by the ZnO nanoparticles giving a homogeneous coverage with more adsorption active sites.

The FTIR analysis was used to characterize and determine the surface functional groups of the adsorbent (Fig. 2). The plant extract showed a broad peak range at 3,200–3,500 cm^{-1} which corresponds to phenolic functional groups as the main stabilizing agents for the ZnO nanoparticles [41]. The strong peak in the range of 1,126–1,190 cm^{-1} indicates carbonyl group related heterocyclic compounds of the plant extracts [42]. The absorption peak observed in the region of 900–1,300 cm^{-1} indicated the phosphorus-containing functional groups resulting from the phosphoric acid activation, used during the preparation process [43]. The broad absorption band observed at 3,471 cm^{-1} represent the O–H stretching vibrations of physically adsorbed water molecules in the ZnO and AC functional group. The peaks at 2,931 and 2,901 cm^{-1} are attributed to the C–H stretching of the methyl groups. The vibration band at 1,780 cm^{-1} corresponds to the C=O stretching of the carbonyl group [44]. The absorption bands at 1,627 cm^{-1} represent C=C groups (carbonization). Also, the minor bands observed at 615–617 cm^{-1} indicating aromatic compounds of alkanes in the AC-ZnO composite [42]. In addition to the bands mentioned above, the peak at 655 cm^{-1} confirms the presence of the ZnO nanoparticles [45]. Some small peaks were also disappeared in the AC-ZnO indicating the ZnO nanoparticles coating on the AC.

The XRD pattern for the adsorbent at angle 2θ has been shown to determine the crystalline phase and structural properties of the nanoparticles. The results of this analysis
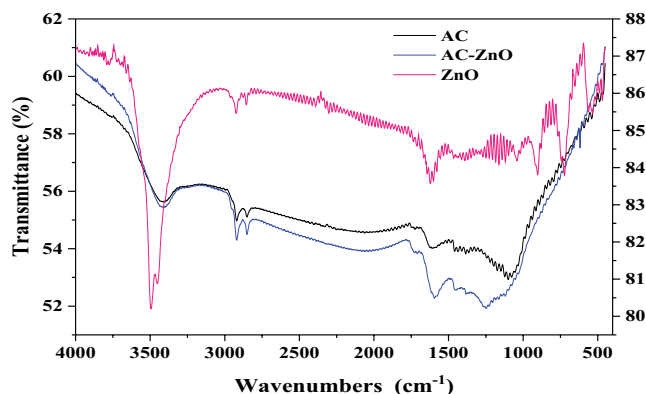

Fig. 2. FTIR spectra of the AC, ZnO and AC-ZnO.

showed that the peaks produced in 31.75°, 34.45°, 36.32°, 47.52°, 59.6°, 62.85°, 66.45°, 67.95°, and 69.15° degrees were the indicators of ZnO in the structure of the synthesized adsorbent (Fig. 3). Moreover, the formation of sharpened and pulled peaks at angles 23.61°, 24.1°, and 26.5° was related to carbon, hence it could be stated that ZnO was successfully synthesized [46].

The nitrogen adsorption/desorption isotherms were applied to characterize the BET specific surface area, pore-volume, and pore size of the non-modified and modified AC. Fig. 4 depicts the N$_2$ adsorption/desorption isotherms of the AC and AC-ZnO. The isotherms were categorized as type IV according to the IUPAC isotherm hysteresis loops, which proves the existence of mesopores in both adsorbents at high pressures (p/p_0 > 4). In addition, according to Fig. 3, as the relative amount of the ZnO nanoparticles increased, the mesopore volume fraction also steadily increased. The obtained results of BET for the AC and AC-ZnO have been shown in Table 2. As can
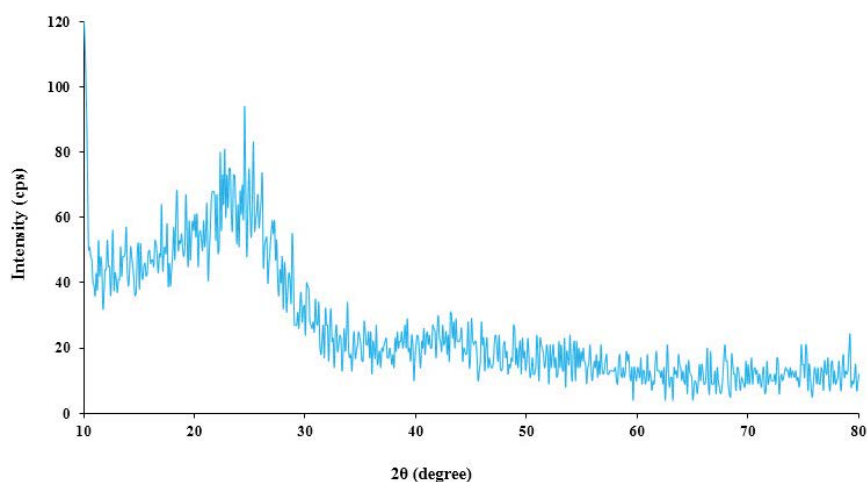
Fig. 3. XRD spectrum of AC and AC-ZnO adsorbents.

Table 2
BET specific surface area (S_{BET}), micropore specific surface area (S_{micro}), mesopore specific surface area (S_{meso}), total pore volume (V_{Total}), micropore volume (V_{micro}), mesopore volume (V_{meso}) and pore diameter (D_p) of the AC and AC-ZnO

Material	S_{BET} (m²/g)	S_{micro} (m²/g)	S_{meso} (m²/g)	V_{Total} (cm³/g)	V_{micro} (cm³/g)	V_{meso} (cm³/g)	D_p (nm)
AC	345.87	222.16	123.71	0.3976	0.0878	0.3098	3.01
AC-ZnO	391.11	235.87	155.24	0.4166	0.0914	0.3187	3.14

be seen, the AC-ZnO has better property than the AC in all parameters, particularly in surface area. The specific surface area, pore volume and pore size of the AC-ZnO were 345.87 m²/g, 0.3976 m²/g and 3.01 nm, respectively. The result confirms that the modified AC by the ZnO nanoparticles has smaller-sized nanoparticles and possesses a high specific surface area, which is suitable for the adsorption of pollutants.

3.2. Effect of operational parameters on dye removal

3.2.1. Solution pH

The pH of the solution and the point of zero charge play an important role in the adsorption process, especially for dye adsorption. The pH of the solution controls the magnitude of electrostatic charges imparted by ionized dye molecules. Therefore, the adsorption efficiency varies with the pH of the medium used [47,48]. The effect of pH on AB1 dye removal by the AC-ZnO from solution was studied under identical conditions. The results have been presented in Figs. 5a and b. It is indicated that the maximum dye removal with 74.29% efficiency was observed at pH 3. With increasing pH, the adsorption capacity declined and the efficiency was achieved 40.61% at pH 11, which may be explained by the surface charge of the AC-ZnO. AB1 dye has negatively charged due to the presence of sulfonate group in its structure, as shown in Fig. 1. When AB1 is dissolved in an aqueous solution, the sulfonate groups on its structure are dissociated and converted to anionic ions [49]. At acidic pH, the surface of the AC-ZnO becomes protonated and its surface charge becomes positive, which
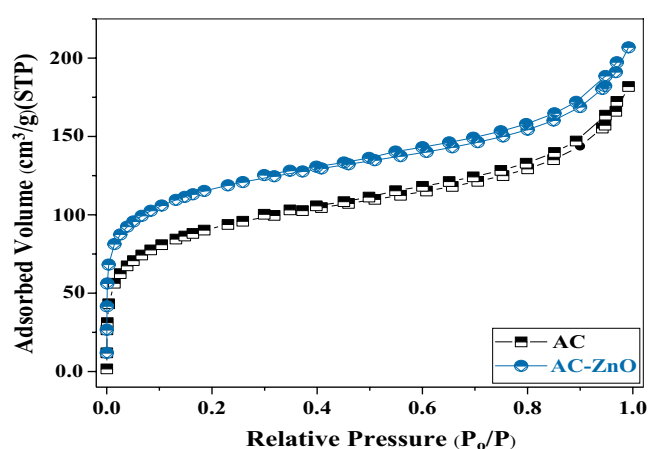

Fig. 4. N$_2$ adsorption–desorption isotherms of the AC and AC-ZnO.

is suitable for adsorbing anionic dyes, and the removal efficiency of AB1 dye enhanced [50]. As the pH of the solution increased, the number of negatively charged sites on the adsorbent surface went up, which is not suitable for anionic dye adsorption [51]. In addition, large quantities of hydroxide ions (OH⁻) present at alkaline pH compete with dye molecules for adsorption on the active sites [52].

Thus, electrostatic interaction is the major adsorption mechanism. ACs are amphoteric substances that can have a positive or negative surface charge, and therefore the pH of the solution affects adsorbent charge and electrostatic interactions between the dye and AC-ZnO [53]. The
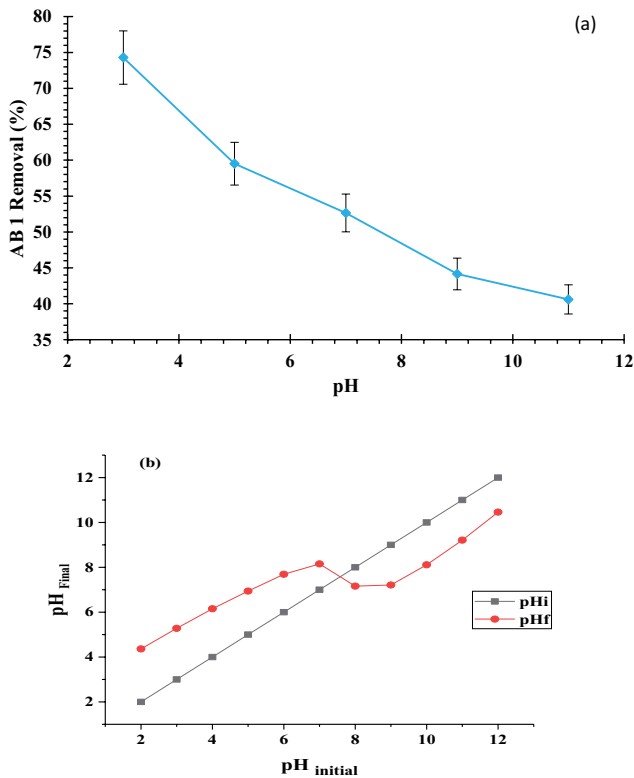
Fig. 5. Effect of pH on the removal of AB1 (contact time: 30 min; initial dye concentration: 100 mg/L; solution temperature: 25°C; AC-ZnO dose: 1 g/L (a) and pH_{pzc} (b)).

pH_{pzc} for the AC-ZnO was determined in order to estimate the ranges where the surface charge is positive. Fig. 4b shows the Zeta potential of the AC-ZnO. It is noticed that the pH_{pzc} of the AC-ZnO corresponds to the solution pH value of 7.16. The surface of the adsorbent has a net positive charge at pH values lower than pH_{pzc} (pH < pH_{pzc}), while, at pH values higher than pH_{pzc} (pH > pH_{pzc}), the surface becomes negatively charged. Thus, at pH below 7.16 (pH < 7.16), due to the electrostatic attraction forces between the positively charged of the AC-ZnO adsorbent surface and negatively charged of anionic dye, higher adsorption efficiency is expected. Similar behavior has been reported in the literature for the adsorption of anionic dyes [54,55] and ionic dye-activated carbon cloth systems [56].

3.2.2. Adsorbent dose

The study of the effect of adsorbent dose provides information on the effectiveness of the adsorbent and the ability to remove one type of contaminant with a minimum dosage, which is suitable for its wide range of applications [57]. In this study, some experiments were conducted at various doses (0.25–2 g/L) to determine the effect of adsorbent dose on the uptake of AB1 dye by the AC-ZnO. As can be observed from Fig. 6, with increasing the adsorbent dose from 0.25 to 1.5 g/L, the percentage of dye removal increased significantly. Because, as the amount of adsorbent increases, the number of active sites on the surface of the adsorbent and

its specific surface area increases [58,59]. However, no significant change was observed in dye removal efficiency at higher adsorbent doses. This phenomenon can be attributed to the overlapping or aggregation of adsorption sites [60]. It should be pointed out that, at doses of 1.5 and 2 g/L, the dye removal rates were 93.4% and 95.7%, respectively. Thus, 1.5 g/L of the AC-ZnO dosage was sufficient for the adsorption of AB1 dye.

Moreover, Fig. 6 shows that with raising the adsorbent dose from 0.25 to 2 g/L the absorption capacity reduced from 112.16 to 47.85 mg/g. This may be due to the crowding of adsorbent particles which leads to overlap or accumulation of adsorption sites, resulting in a decrease in surface area and accordingly an increase in propagation path length [61]. Similar behavior of adsorption parameters against the adsorbent dose was reported by Rehman et al. [61].

3.2.3. Initial dye concentration

The effect of initial AB1 dye concentration was investigated over the range of 100–350 mg/L, while other parameters were kept constant. The effect of initial AB1 concentration on the sorption efficiency and adsorption capacity has been given in Fig. 7. It was found that the adsorption efficiency and adsorption capacity had opposite trends against increasing initial dye concentration. With raising initial dye concentration, the efficiency of dye removal decreased from 97.79 to 43.87 mg/L while the adsorption capacity increased from 65.19 to 102.37 mg/g. This phenomenon can be described as, at low concentrations, the ratio of the number of dye molecules to the number of active sites available at the adsorbent surface is lower; as a result, dye molecules have a more opportunity to reach active sites and, in turn, the uptake efficiency is higher. The rate of AB1 adsorption decreased with increasing initial dye concentration, because the adsorbent sites are occupied by dye molecules and they compete with each other for the fixed number of binding sites, thus, the sufficient active sites required for AB1 adsorption was not available at higher initial concentrations [62,63]. The increased adsorption capacity at higher initial dye contents can be attributed to enhanced driving force leading to an increase in the rate of dye diffusion [64]. A similar trend of Direct Red-31 and Direct Orange-26 dyes adsorption efficiency and adsorption capacity of rice husk against the initial concentration was reported by Safa and Bhatti [65].

3.2.4. Contact time and initial dye concentration

The effect of contact time on the adsorption of AB1 dye by the AC-ZnO was examined at different initial AB1 dye concentrations of 25, 50, 100, 150 mg/L and different time intervals of 2, 4, 6, 8, 10, 15, 30, 45, 60 and 90 min while other parameters were kept constant (Fig. 8). It can be easily observed that the adsorption efficiency of AB1 dye by the AC-ZnO decreased with increasing initial dye concentration. At lower concentrations, the dye was rapidly adsorbed on the AC-ZnO adsorbent, but active sites on the AC-ZnO surface were occupied gradually with increasing dye concentration, thereby creating a repulsive force between the dye molecules in the solution and on the
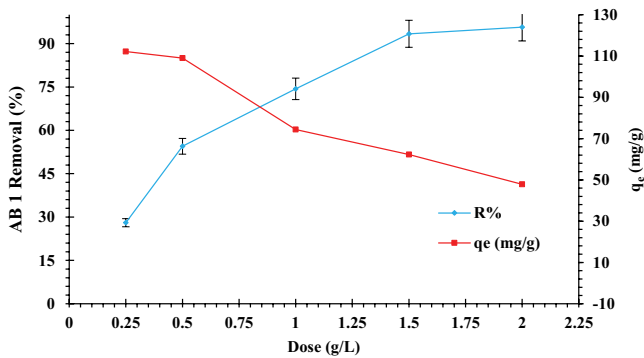
Fig. 6. Effect of adsorbent dose on the removal of AB1 dye (pH: 3; contact time: 30 min; initial dye concentration: 100 mg/L; solution temperature: 25°C).
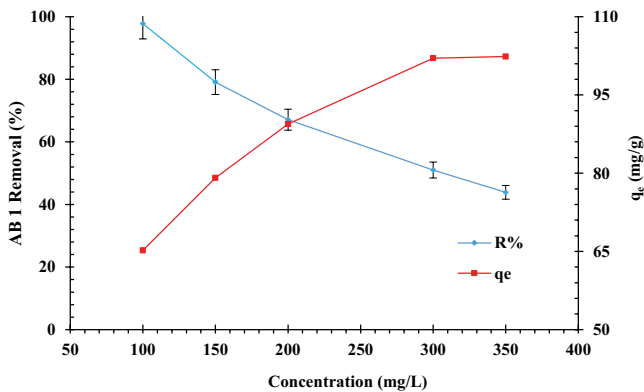

Fig. 7. Effect of changes in initial dye concentration on the removal of AB1 dye (pH: 3; AC-ZnO: 1.5 g/L; pH: 3; contact time: 60 min).
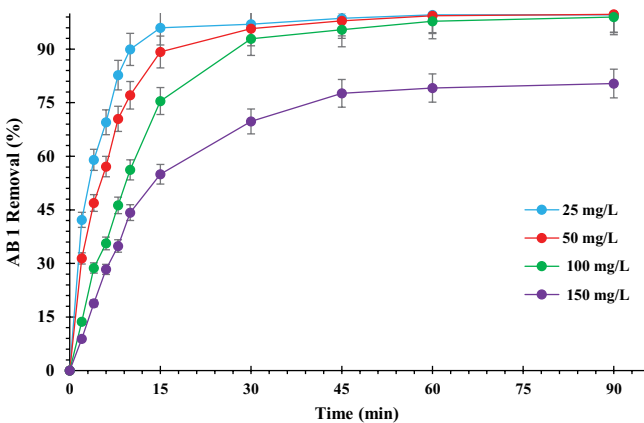

Fig. 8. Effect of contact time on the removal of AB1 dye (AC-ZnO: 1.5 g/L; pH: 3; contact time: 30 min).

adsorbent surface [66]. Therefore, the repulsive force leads to reducing the dye adsorption. Moreover, the adsorption process was very fast in the early phase, and then gradually increased until the equilibrium. The equilibrium was attained within 60 min for 25 mg/L of dye concentration, and for other concentrations achieved 90 min. In the rapid phase, many vacant sites are available on the sorbent

and adsorption is fast, whereas, with the occupation of these sites, the driving force decreases, causing the rate of adsorption to decrease [63,67]. Similar observations have also been reported by other researchers [68–70].

3.2.5. Isotherm modeling

The adsorption isotherm is the amount of pollution which is adsorbed per unit mass of an adsorbent as a function of equilibrium concentration. Various isotherm models have been used to evaluate dye adsorption mechanism such as Langmuir, Freundlich, Dubinin–Radushkevich, Redlich–Peterson, Sips, and Temkin, the most common of which are Langmuir and Freundlich [71,72]. The Langmuir isotherm describes monolayer adsorption at specific homogeneous adsorption sites with the identical sorption energies, and the interaction among adsorbed molecules can be negligible [73,74]. The linear form of the Langmuir isotherm equation can be represented as follows:

$$\frac{1}{q_e} = \frac{1}{q_{max}} + \frac{1}{bq_{max}}\frac{1}{C_e} \tag{3}$$

where q_e is the equilibrium dye concentration on the adsorbent (mg/g), C_e is the equilibrium concentration of the dye in solution (mg/L), q_{max} is the maximum monolayer capacity of the adsorbent (mg/g) and b is the adsorption equilibrium Langmuir constant (L/mg) [75]. The Freundlich isotherm model assumes multi-layer adsorption and heterogeneous pollution on the adsorbent surface [76]. Its linear form can be as follows:

$$\log q_e = \log K_F + \frac{1}{n}\log C_e \tag{4}$$

where q_e and C_e are the same as mentioned above; K_F is the Freundlich constant (mg/g)(L/mg)$^{1/n}$ and n is heterogeneity factor.

The graph of the Langmuir and Freundlich isotherms has been presented in Fig. 9. Also, the calculated values for the isotherm parameters have been indicated in Table 3. The value of the correlation coefficients (R^2) for the Freundlich isotherm was 0.9622 which is close to 1 and higher than the Langmuir isotherm (0.7882). Thus, the Freundlich model was suitable for adsorption isotherm data, and it confirmed that a multilayer AB1 dye adsorption occurred on the heterogeneous surfaces of the AC-ZnO. The value of heterogeneity factor (n) should be between 1 and 10 and as the slope $1/n$ gets closer to zero, the surface becomes more heterogeneous [71]. In this study, the n value was estimated at 9.62 and the $1/n$ value was closed to 0, which represents the heterogeneous adsorbent surface and the existing high energy sites on the surface of the AC-ZnO [67]. Similar isotherm results were obtained for various pollutant-activated carbon systems in the literature [77,78].

Also, the adsorption capacity of the AC-ZnO for AB1 removal was 93.46 mg/g, illustrating a relatively good adsorption capacity compared to the AC prepared from

Table 3
Values of isotherm parameters for AB1 dye adsorption on AC-ZnO

Isotherm	Isotherm parameter	Value
Langmuir	q_{max} (mg/g)	93.46
	b (L/mg)	1.009
	R^2	0.7882
Freundlich	K_F (mg/g)(L/mg)$^{1/n}$	58.60
	n	9.62
	R^2	0.9622

and predicate the rate-controlling step. They are given by equations [86]:

$$\text{Pseudo-first-order model: } \log\left(q_e - q_t\right) = \log q_e - \frac{k_1}{2.303}t \quad (5)$$

$$\text{Pseudo-second-order model: } \frac{t}{q_t} = \frac{1}{k_2 q_e^2} + \frac{t}{q_e} \quad (6)$$

where q_e is the amount of dye adsorbed (mg/g) at equilibrium, q_t is the amount of dye adsorbed at time t (min). k_1 and k_2 are the rate constant of adsorption of the pseudo-first-order and pseudo-second-order models, respectively. The values of the rate constant (k_1 and k_2), and q_e were determined from the linear plots of the graph and the values have been given in Fig. 10 and Table 5.

Based on the results, the correlation coefficient (R^2) value is relatively higher for the pseudo-second-order than the pseudo-first-order model which suggests that the adsorption of AB1 onto the AC-ZnO obeyed the pseudo-second-order model. Therefore, the adsorption process involves chemical and electrostatic interaction mechanisms between the dye molecules and the functional groups on the surface of the AC-ZnO [87]. The maximum value of q_e (92.59 mg/g) calculated from the pseudo-second-order model was close to q_m which was determined from the Langmuir equation (93.46 mg/g), confirming the system compliance with the pseudo-second-order model. Furthermore, the k_2 value decreased, as the initial dye concentration increased, which may be due to low competition for adsorption on active
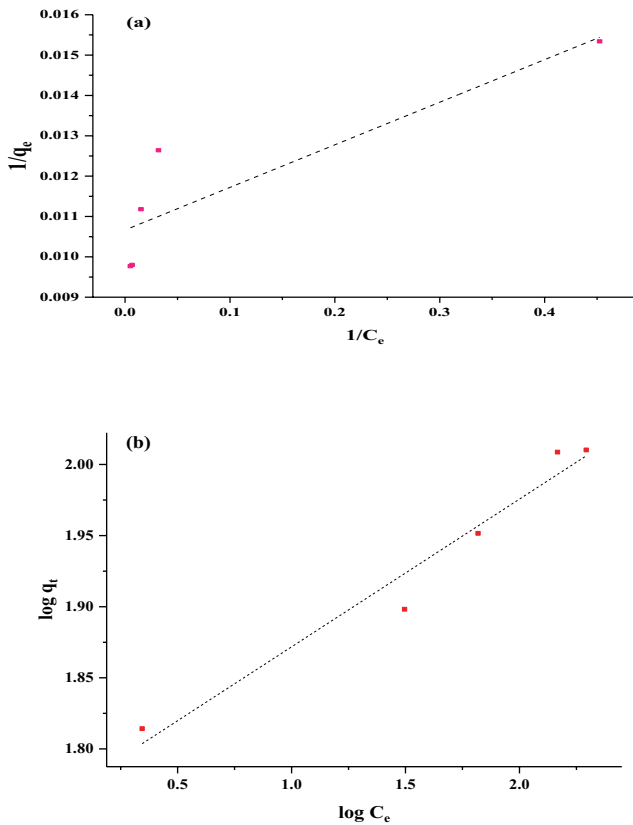
Fig. 9. Langmuir (a) and Freundlich isotherm plots (b) for AB1 dye adsorption on the AC-ZnO.

scrap tires (14.51 mg/L) reported by Hoseinzadeh et al. for AB1 adsorption [79]. A comparison between the adsorption capacity of AC-ZnO and other adsorbents for AB1 is shown in Table 4. Based on this comparison, AC-ZnO has a relatively high adsorption capacity compared to other adsorbents reported in the literature, suggesting that it is a promising adsorbent for anionic dye removal from wastewater.

3.2.6. Kinetic study

The pseudo-first-order and pseudo-second-order models are used to demonstrate the regular adsorption pattern

Table 4
Comparison of AB1 adsorption capacity of AC-ZnO with other reported adsorbents

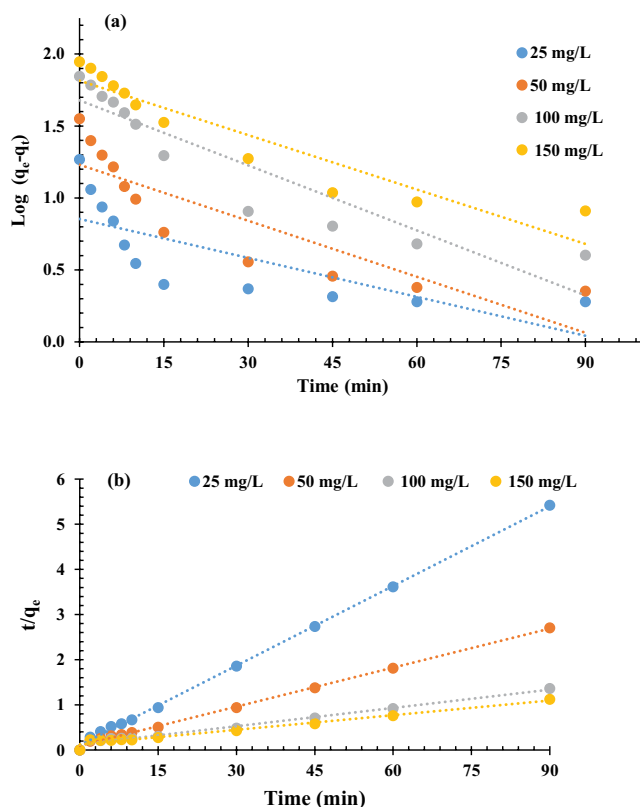| Adsorbents	Adsorption capacity (mg/g)	References
Lignocellulosic waste biomass activated carbon	3.8	[80]
Fly ash	18.9	[81]
Cerastoderma lamarcki shell	20.894	[82]
Brown algae	27.2–29.6	[83]
Nizamuddin zanardini	29.79	[84]
Sargassum glaucescens	27.19	[84]
Stochospermum marginatum	29.56	[84]
Spent bleaching earth modified by CTAB	100	[85]
AC-ZnO	93.46	This study

Fig. 10. Pseudo-first-order (a) and pseudo-second-order kinetics plots (b) for AB1 dye adsorption on the AC-ZnO.

sites at lower concentrations, resulting in a faster rate of dye adsorption [88], which was similar to the observations by Fathi et al. [89] and Zhang et al. [90].

3.2.7. Thermodynamic study

The thermodynamic parameters are useful for determining whether the adsorption process is endothermic or exothermic, as well as and spontaneous or non-spontaneous. Three thermodynamic parameters including standard enthalpy change ($\Delta H°$), standard Gibbs free energy change ($\Delta G°$) and standard entropy change ($\Delta S°$) were interpreted to study the thermodynamic behavior. The values of $\Delta H°$ and $\Delta S°$ were calculated using the following equations [91].

$$\Delta G° = -RT \ln K_c \tag{7}$$

$$K_c = \frac{q_e}{C_e} \tag{8}$$

where T (K) is the soluble temperature, R (8.314 J/mol K) is the universal gas constant and K_c (L/g) is the equilibrium constant, and q_e and C_e are the equilibrium concentrations of AB1 on AC-ZnO (mg/g) and in the solution (mg/L), respectively. The thermodynamic parameters, $\Delta H°$ and $\Delta S°$, are calculated from the slope and intercept of plot $\log K_c$ vs. $1/T$, respectively. The values of $\Delta G°$ can also be calculated from the following equation:

$$\Delta G° = \Delta H° - T\Delta S° \tag{9}$$

The thermodynamic parameters of AB1 adsorption on AC-ZnO have been shown in Table 6. According to the results, the positive value for $\Delta H°$ indicates that the adsorption process of AB1 was endothermic, which is a strong reason for the strong interaction between AC-ZnO and AB1. Moreover, the negative $\Delta S°$ values illustrate a decrease in the irregularity in the reaction as well as a decrease in the efficiency of temperature rise in the solid–liquid phase during the adsorption process. Also, the positive $\Delta G°$ obtained for different temperatures reflects the fact that the reaction is non-spontaneous [91].

The findings showed that raising temperature led to an increase in adsorption. This is due to the fact that an increase in temperature may cause better and faster penetration of the adsorbate molecules among the outer layer and the inner pores of the adsorbent particles. Moreover, an increase in temperature promoted the mobility of the dye molecules, thereby increasing the contact of the dye with active sites on the adsorbent, which resulted in an increased dye adsorption rate [92,93].

3.2.8. Regeneration of AC-ZnO

The regeneration of adsorbent is one of the crucial factors for the application of an adsorbent that substantially influences cost and emissions [90]. Here, the reusability of the adsorbent was evaluated by repeated regeneration via washing adsorbent using 0.1 M NaOH solution and deionized water. After the regeneration, the adsorbent was used again to remove the dye. The results have been presented in Fig. 11. As can be seen, under the optimum conditions, the adsorption efficiency for AB1 removal was 92.88% and reached 66.87% after four cycles. The findings revealed that

Table 5
The values of kinetic parameters for AB1 dye adsorption on the AC-ZnO

Dye concentration (mg/L)	$q_{e,\text{epx}}$ (mg/g)	Pseudo-first-order			Pseudo-second-order		
		$q_{1,\text{cal}}$ (mg/g)	k_1 (1/min)	R^2	$q_{2,\text{cal}}$ (mg/g)	k_2 (g mg/min)	R^2
25	18.5	7.15	0.0207	0.5696	17.06	0.0330	0.9991
50	35.5	17.01	0.0299	0.7572	34.72	0.0086	0.9976
100	70	47.70	0.0348	0.8592	74.07	0.0015	0.982
150	88.5	65.34	0.0290	0.8809	92.59	0.0010	0.9736

Table 6
Thermodynamic parameters for AB1 adsorption on AC-ZnO

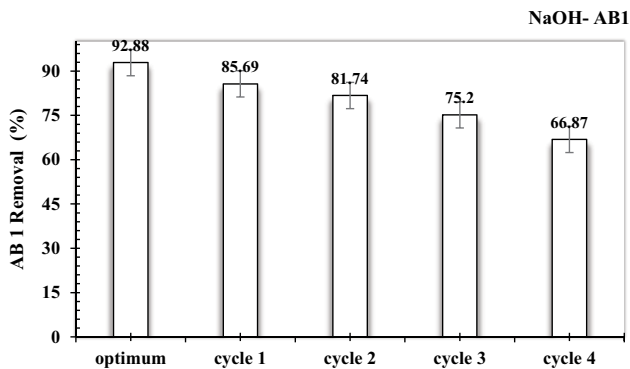| Temperature (K)	$\Delta G°$ (kJ/mol)	$\Delta S°$ (kJ/mol K)	$\Delta H°$ (kJ/mol)
283	53.980		
298	55.419	–0.09594	26.815
313	56.858		

Fig. 11. Reusability of the AC-ZnO after five consecutive adsorption–desorption cycles (dye concentration: 100 mg/L; adsorbent dose: 1.5 g/L; pH: 3; contact time: 30 min).

the AC-ZnO could easily be regenerated and still retained its high adsorption capacity after at least four cycles.

3.2.9. Application of AC-ZnO using real samples

Further investigation of the removal of AB1 onto the AC-ZnO was performed by means of the real wastewater samples. The samples were obtained from the Sivan Textile Company in Ardabil. The treatment was subjected to the AC-ZnO under optimized adsorption conditions. It should be noted that the samples contained a large variety of other contaminants which could compete with the target contaminants for the adsorption sites. However, the results showed that the AC-ZnO still had significant efficiency of dye removal (71.21%). This observation suggests that the AC-ZnO has a good potential for the removal of dyes in real samples. Generally, using the AC-ZnO as a low-cost and environmentally friendly adsorbent can be a cost-effective and useful method for AB1 dye removal.

4. Conclusion

In this study, worn tire specimens were used as abundant raw material for the production of AC and were modified with the ZnO nanoparticles obtained from the pomegranate peel extract to prepare the AC-ZnO. The characterization of the synthesized adsorbent demonstrated that the AC-ZnO was successfully synthesized. The pH values of dye solution control the adsorption process and the highest efficiency (74.29%) and adsorption capacity (93.46 mg/g) of the AC-ZnO for AB1 was observed at pH 3. The adsorption was well described by the pseudo-second-order model and

the equilibrium data were best fitted to the Freundlich isotherm model. The AC-ZnO could be regenerated and reused for several cycles for AB1 dye removal and was also effective in removing dye from actual textile wastewater. The present study showed that the AC-ZnO could be employed effectively as a low-cost and environmentally benign adsorbent for the removal of AB1 dye from colored wastewaters.

Acknowledgments

References

[1] R. Khosravi, M. Fazlzadehdavil, B. Barikbin, H. Hossini, Electro-decolorization of Reactive Red 198 from aqueous solutions using aluminum electrodes systems: modeling and optimization of operating parameters, Desal. Water Treat., 54 (2015) 3152–3160.
[2] A.R. Rahmani, A. Shabanloo, M. Fazlzadeh, Y. Poureshg, H. Rezaeivahidian, Degradation of Acid Blue 113 in aqueous solutions by the electrochemical advanced oxidation in the presence of persulfate, Desal. Water Treat., 59 (2017) 202–209.
[3] A. Rahmani, J. Mehralipor, N. Shabanloo, F. Zaheri, Y. Poreshg, A. Shabanloo, Performance evaluation of advanced electrochemical oxidation process with the using persulfate in degradation of acid blue 113 from aqueous solutions, J. Sabzevar Univ. Med. Sci., 21 (2014) 797–807.
[4] S.M. Stagnaro, C. Volzone, L. Huck, Nanoclay as adsorbent: evaluation for removing dyes used in the textile industry, Procedia Mater. Sci., 8 (2015) 586–591.
[5] S. Tunç, O. Duman, T. Gürkan, Monitoring the decolorization of Acid Orange 8 and Acid Red 44 from aqueous solution using Fenton's reagents by online spectrophotometric method: effect of operation parameters and kinetic study, Ind. Eng. Chem. Res., 52 (2013) 1414–1425.
[6] C.-Z. Liang, S.-P. Sun, F.-Y. Li, Y.-K. Ong, T.-S. Chung, Treatment of highly concentrated wastewater containing multiple synthetic dyes by a combined process of coagulation/flocculation and nanofiltration, J. Membr. Sci., 469 (2014) 306–315.
[7] R. Khosravi, S. Hazrati, M. Fazlzadeh, Decolorization of AR18 dye solution by electrocoagulation: sludge production and electrode loss in different current densities, Desal. Water Treat., 57 (2016) 14656–14664.
[8] A.R. Rahmani, A. Shabanloo, M. Fazlzadeh, Y. Poureshg, Investigation of operational parameters influencing in treatment of dye from water by electro-Fenton process, Desal. Water Treat., 57 (2016) 24387–24394.
[9] A. Seid-Mohammadi, A. Shabanloo, M. Fazlzadeh, Y. Poureshg, Degradation of acid blue 113 by US/H_2O_2/Fe^{2+} and US/$S_2O_8^{2-}$/Fe^{2+} processes from aqueous solutions, Desal. Water Treat., 78 (2017) 273–280.
[10] M.T. Samadi, S. Ahmadi, Y. Poureshg, A. Shabanloo, Z. Rahmani, M. Vanaei Tabar, Efficiency of Mn^{2+}/H_2O_2 process in removal of Reactive blue 19 dyes from aquatic environments, J. Environ. Occup. Health, 2 (2017) 247–258.
[11] C. Li, T. Lou, X. Yan, Y.-z. Long, G. Cui, X. Wang, Fabrication of pure chitosan nanofibrous membranes as effective absorbent for dye removal, Int. J. Biol. Macromol., 106 (2018) 768–774.
[12] S.M. Seyed Arabi, R.S. Lalehloo, M.R.T.B. Olyai, G.A.M. Ali, H. Sadegh, Removal of congo red azo dye from aqueous solution by ZnO nanoparticles loaded on multiwall carbon nanotubes, Physica E, 106 (2019) 150–155.
[13] K.A. Abdulsalam, A.A. Giwa, Adsorptive de-colouration of textile wastewater using an acid-modified sawdust, ChemSearch J., 9 (2018) 13–18.
[14] R. Khosravi, H. Eslami, A. Zarei, M. Heidari, A.N. Baghani, N. Safavi, A. Mokammel, M. Fazlzadeh, S. Adhami, Comparative

evaluation of nitrate adsorption from aqueous solutions using green and red local montmorillonite adsorbents, Desal. Water Treat., 116 (2018) 119–128.

[15] H. Abdoallahzadeh, B. Alizadeh, R. Khosravi, M. Fazlzadeh, Efficiency of EDTA modified nanoclay in removal of humic acid from aquatic solutions, J. Mazandaran Univ. Med. Sci., 26 (2016) 111–125.

[16] G.F.O. do Nascimento, G.R.B. da Costa, C.M.B. de Araújo, M.G. Ghislandi, M.A. da Motta Sobrinho, Graphene-based materials production and application in textile wastewater treatment: color removal and phytotoxicity using *Lactuca sativa* as bioindicator, J. Environ. Sci. Health. Part A Toxic/Hazard. Subst. Environ. Eng., 55 (2020) 97–106.

[17] S. Uçar, M. Erdem, T. Tay, S. Karagöz, Preparation and characterization of activated carbon produced from pomegranate seeds by $ZnCl_2$ activation, Appl. Surf. Sci., 255 (2009) 8890–8896.

[18] O. Ioannidou, A. Zabaniotou, Agricultural residues as precursors for activated carbon production—a review, Renewable Sustainable Energy Rev., 11 (2007) 1966–2005.

[19] E.A. Deliyanni, Chapter 5 - Low-cost Activated Carbon from Rice Wastes in Liquid-phase Adsorption, Interface Sci. Technol., 30 (2019) 101–123.

[20] J.M.V. Nabais, C.E.C. Laginhas, P.J.M. Carrott, M.M.L. Ribeiro Carrott, Production of activated carbons from almond shell, Fuel Process. Technol., 92 (2011) 234–240.

[21] K.T. Wong, N.C. Eu, S. Ibrahim, H. Kim, Y. Yoon, M. Jang, Recyclable magnetite-loaded palm shell-waste based activated carbon for the effective removal of methylene blue from aqueous solution, J. Cleaner Prod., 115 (2016) 337–342.

[22] F. Gündüz, B. Bayrak, Biosorption of malachite green from an aqueous solution using pomegranate peel: equilibrium modelling, kinetic and thermodynamic studies, J. Mol. Liq., 243 (2017) 790–798.

[23] F.R. Qin, K. Zhang, J. Li, Y.Q. Lai, H. Lu, W.W. Liu, F. Yu, X.K. Lei, J. Fang, Pomegranate rind-derived activated carbon as electrode material for high-performance supercapacitors, J. Solid State Electrochem., 20 (2016) 469–477.

[24] R.A. de Toledo, U.H. Chao, T.T. Shen, Q.H. Lu, X.Q. Li, H. Shim, Development of hybrid processes for the removal of volatile organic compounds, plasticizer, and pharmaceutically active compound using sewage sludge, waste scrap tires, and wood chips as sorbents and microbial immobilization matrices, Environ. Sci. Pollut. Res., 26 (2019) 11591–11604.

[25] F. Jahanbakhsh, B. Ebrahimi, Modified activated carbon with zinc oxide nanoparticles produced from used tire for removal of Acid Green 25 from aqueous solutions, Am. J. Appl. Chem., 4 (2016) 8–13.

[26] V.K. Gupta, M.R. Ganjali, A. Nayak, B. Bhushan, S. Agarwal, Enhanced heavy metals removal and recovery by mesoporous adsorbent prepared from waste rubber tire, Chem. Eng. J., 197 (2012) 330–342.

[27] E. Babiker, M.A. Al-Ghouti, N. Zouari, G. McKay, Removal of boron from water using adsorbents derived from waste tire rubber, J. Environ. Chem. Eng., 7 (2019) 102948, doi: 10.1016/j.jece.2019.102948.

[28] T.A. Saleh, K.R. Alhooshani, M.S.A. Abdelbassit, Evaluation of AC/ZnO composite for sorption of dichloromethane, trichloromethane and carbon tetrachloride: kinetics and isotherms, J. Taiwan Inst. Chem. Eng., 55 (2015) 159–169.

[29] M.Y. Nassar, M.M. Moustafa, M.M. Taha, Hydrothermal tuning of the morphology and particle size of hydrozincite nanoparticles using different counterions to produce nanosized ZnO as an efficient adsorbent for textile dye removal, RSC Adv., 6 (2016) 42180–42195.

[30] C. Mason, S. Vivekanandhan, M. Misra, A.K. Mohanty, Switchgrass (*Panicum virgatum*) extract mediated green synthesis of silver nanoparticles, World J. Nano Sci. Eng., 2 (2012) 47–52.

[31] M. Fazlzadeh, R. Khosravi, A. Zarei, Green synthesis of zinc oxide nanoparticles using *Peganum harmala* seed extract, and loaded on *Peganum harmala* seed powdered activated carbon

[32] P. Jamdagni, P. Khatri, J. Rana, Green synthesis of zinc oxide nanoparticles using flower extract of *Nyctanthes arbor-tristis* and their antifungal activity, J. King Saud Univ. Sci., 30 (2018) 168–175.

[33] D. Suresh, P.C. Nethravathi, Udayabhanu, H. Rajanaika, H. Nagabhushana, S.C. Sharma, Green synthesis of multifunctional zinc oxide (ZnO) nanoparticles using *Cassia fistula* plant extract and their photodegradative, antioxidant and antibacterial activities, Mater. Sci. Semicond. Process., 31 (2015) 446–454.

[34] N. Bala, S. Saha, M. Chakraborty, M. Maiti, S. Das, R. Basu, P. Nandy, Green synthesis of zinc oxide nanoparticles using *Hibiscus subdariffa* leaf extract: effect of temperature on synthesis, anti-bacterial activity and anti-diabetic activity, RSC Adv., 5 (2015) 4993–5003.

[35] K. Elumalai, S. Velmurugan, S. Ravi, V. Kathiravan, S. Ashokkumar, Retracted: green synthesis of zinc oxide nanoparticles using *Moringa oleifera* leaf extract and evaluation of its antimicrobial activity, Spectrochim. Acta, Part A, 143 (2015) 158–164.

[36] Qurrat-ul-Ain, J. Khatoon, M.R. Shah, M.I. Malik, I.A.T. Khan, S. Khurshid, R. Naz, Convenient pH-responsive removal of Acid Black 1 by green L-histidine/iron oxide magnetic nanoadsorbent from water: performance and mechanistic studies, RSC Adv., 9 (2019) 2978–2996.

[37] Y. Rashtbari, S. Hazrati, A. Azari, S. Afshin, M. Fazlzadeh, M. Vosoughi, A novel, eco-friendly and green synthesis of PPAC-ZnO and PPAC-nZVI nanocomposite using pomegranate peel: cephalexin adsorption experiments, mechanisms, isotherms and kinetics, Adv. Powder Technol., 31 (2020) 1612–1623.

[38] H. Abdollahzadeh, M. Fazlzadeh, S. Afshin, H. Arfaeinia, A. Feizizadeh, Y. Poureshgh, Y. Rashtbari, Efficiency of activated carbon prepared from scrap tires magnetized by Fe_3O_4 nanoparticles: characterisation and its application for removal of reactive blue 19 from aquatic solutions, Int. J. Environ. Anal. Chem., (2020) 1745199 (1–15), doi: 10.1080/03067319.2020.1745199.

[39] R. Shokoohi, M.T. Samadi, M. Amani, Y. Poureshgh, Modeling and optimization of removal of cefalexin from aquatic solutions by enzymatic oxidation using experimental design, Braz. J. Chem. Eng., 35 (2018) 943–956.

[40] N. Subedi, A. Lähde, E. Abu-Danso, J. Iqbal, A. Bhatnagar, A comparative study of magnetic chitosan ($Chi@Fe_3O_4$) and graphene oxide modified magnetic chitosan ($Chi@Fe_3O_4GO$) nanocomposites for efficient removal of Cr(VI) from water, Int. J. Biol. Macromol., 137 (2019) 948–959.

[41] N. Matinise, X.G. Fuku, K. Kaviyarasu, N. Mayedwa, M. Maaza, ZnO nanoparticles via *Moringa oleifera* green synthesis: physical properties & mechanism of formation, Appl. Surf. Sci., 406 (2017) 339–347.

[42] M. Fazlzadeh, K. Rahmani, A. Zarei, H. Abdoallahzadeh, F. Nasiri, R. Khosravi, A novel green synthesis of zero valent iron nanoparticles (NZVI) using three plant extracts and their efficient application for removal of Cr(VI) from aqueous solutions, Adv. Powder Technol., 28 (2017) 122–130.

[43] M.-s. Miao, Q. Liu, L. Shu, Z. Wang, Y.-z. Liu, Q. Kong, Removal of cephalexin from effluent by activated carbon prepared from alligator weed: kinetics, isotherms, and thermodynamic analyses, Process Saf. Environ. Prot., 104 (2016) 481–489.

[44] M. Ghaedi, A. Ansari, M.H. Habibi, A. Asghari, Removal of malachite green from aqueous solution by zinc oxide nanoparticle loaded on activated carbon: kinetics and isotherm study, J. Ind. Eng. Chem., 20 (2014) 17–28.

[45] M. Ramesh, M. Anbuvannan, G. Viruthagiri, Green synthesis of ZnO nanoparticles using *Solanum nigrum* leaf extract and their antibacterial activity, Spectrochim. Acta, Part A, 136 (2015) 864–870.

[46] Y. Rashtbari, S. Afshin, A. Hamzezadeh, M. Abazari, Y. Poureshgh, M. Fazlzadehdavh, Application of powdered

activated carbon coated with zinc oxide nanoparticles prepared using a green synthesis in removal of Reactive Blue 19 and Reactive Black-5: adsorption isotherm and kinetic models, Desal. Water Treat., 179 (2020) 354–367.

[47] L.J. Leng, X.Z. Yuan, G.M. Zeng, J.G. Shao, X.H. Chen, Z.B. Wu, H. Wang, X. Peng, Surface characterization of rice husk bio-char produced by liquefaction and application for cationic dye (Malachite green) adsorption, Fuel, 155 (2015) 77–85.

[48] T.W. Seow, C.K. Lim, Removal of dye by adsorption: a review, Int. J. Appl. Eng. Res., 11 (2016) 2675–2679.

[49] C. Santhosh, E. Daneshvar, P. Kollu, S. Peräniemi, A.N. Grace, A. Bhatnagar, Magnetic $SiO_2@CoFe_2O_4$ nanoparticles decorated on graphene oxide as efficient adsorbents for the removal of anionic pollutants from water, Chem. Eng. J., 322 (2017) 472–487.

[50] S.M. Pormazar, A. Dalvand, Adsorption of Reactive Black 5 azo dye from aqueous solution by using amine-functioned Fe_3O_4 nanoparticles with L-arginine: process optimisation using RSM, Int. J. Environ. Anal. Chem., (2020) 1743278 (1–20), doi: 10.1080/03067319.2020.1743278.

[51] S.M. Pormazar, M.H. Ehrampoush, M.T. Ghaneian, M. Khoobi, P. Talebi, A. Dalvand, Application of amine-functioned Fe_3O_4 nanoparticles with HPEI for effective humic acid removal from aqueous solution: modeling and optimization, Korean J. Chem. Eng., 37 (2020) 93–104.

[52] N.M. Mahmoodi, S. Khorramfar, F. Najafi, Amine-functionalized silica nanoparticle: preparation, characterization and anionic dye removal ability, Desalination, 279 (2011) 61–68.

[53] B. Acevedo, R.P. Rocha, M.F. Pereira, J.L. Figueiredo, C. Barriocanal, Adsorption of dyes by ACs prepared from waste tyre reinforcing fibre. Effect of texture, surface chemistry and pH, J. Colloid Interface Sci., 459 (2015) 189–198.

[54] F.A. Ngwabebhoh, M. Gazi, A.A. Oladipo, Adsorptive removal of multi-azo dye from aqueous phase using a semi-IPN superabsorbent chitosan-starch hydrogel, Chem. Eng. Res. Des., 112 (2016) 274–288.

[55] S. Shekoohiyan, G. Moussavi, S. Mojab, A. Alahabadi, Adsorption of the Reactive Azo dyes onto NH_4Cl-induced activated carbon, Environ. Health Eng. Manage. J., 3 (2016) 1–7.

[56] E. Ayranci, O. Duman, In-situ UV-visible spectroscopic study on the adsorption of some dyes onto activated carbon cloth, Sep. Sci. Technol., 44 (2009) 3735–3752.

[57] N. Tripathi, Cationic and anionic dye adsorption by agricultural solid wastes: a comprehensive review, IOSR J. Appl. Chem., 5 (2013) 91–108.

[58] M. Constantin, I. Asmarandei, V. Harabagiu, L. Ghimici, P. Ascenzi, G. Fundueanu, Removal of anionic dyes from aqueous solutions by an ion-exchanger based on pullulan microspheres, Carbohydr. Polym., 91 (2013) 74–84.

[59] S.M. Pormazar, M.H. Ehrampoush, A. Dalvand, Removal of humic acid from aqueous solution by $Fe_3O_4@L$-arginine magnetic nanoparticle: kinetic and equilibrium studies, Int. J. Environ. Anal. Chem., (2020) 1–16, doi: 10.1080/03067319.2020.1767092.

[60] D. Pathania, S. Sharma, P. Singh, Removal of methylene blue by adsorption onto activated carbon developed from *Ficus carica* bast, Arabian J. Chem., 10 (2017) S1445–S1451.

[61] A. Hebeish, M. Ramadan, E. Abdel-Halim, A. Abo-Okeil, An effective adsorbent based on sawdust for removal of direct dye from aqueous solutions, Clean Technol. Environ. Policy, 13 (2011) 713–718.

[62] M.S. Ur Rehman, M. Munir, M. Ashfaq, N. Rashid, M.F. Nazar, M. Danish, J.-I. Han, Adsorption of Brilliant Green dye from aqueous solution onto red clay, Chem. Eng. J., 228 (2013) 54–62.

[63] R. Huang, Q. Liu, J. Huo, B. Yang, Adsorption of methyl orange onto protonated cross-linked chitosan, Arabian J. Chem., 10 (2017) 24–32.

[64] F.Y. Wang, H. Wang, J.W. Ma, Adsorption of cadmium(II) ions from aqueous solution by a new low-cost adsorbent—bamboo charcoal, J. Hazard. Mater., 177 (2010) 300–306.

[65] Y. Safa, H.N. Bhatti, Kinetic and thermodynamic modeling for the removal of Direct Red-31 and Direct Orange-26 dyes from aqueous solutions by rice husk, Desalination, 272 (2011) 313–322.

[66] A.A. Mohammadi, A. Alinejad, B. Kamarehie, S. Javan, A. Ghaderpoury, M. Ahmadpour, M. Ghaderpoori, Metal-organic framework Uio-66 for adsorption of methylene blue dye from aqueous solutions, Int. J. Environ. Sci. Technol., 14 (2017) 1959–1968.

[67] A.H. Mahvi, A. Dalvand, Kinetic and equilibrium studies on the adsorption of Direct Red 23 dye from aqueous solution using montmorillonite nanoclay, Water Qual. Res. J., 55 (2020) 132–144.

[68] N. Kataria, V.K. Garg, M. Jain, K. Kadirvelu, Preparation, characterization and potential use of flower shaped Zinc oxide nanoparticles (ZON) for the adsorption of Victoria Blue B dye from aqueous solution, Adv. Powder Technol., 27 (2016) 1180–1188.

[69] W.A. Khanday, F. Marrakchi, M. Asif, B.H. Hameed, Mesoporous zeolite–activated carbon composite from oil palm ash as an effective adsorbent for methylene blue, J. Taiwan Inst. Chem. Eng., 70 (2017) 32–41.

[70] O. Duman, C. Özcan, T.G. Polat, S. Tunç, Carbon nanotube-based magnetic and non-magnetic adsorbents for the high-efficiency removal of diquat dibromide herbicide from water: OMWCNT, OMWCNT-Fe_3O_4 and OMWCNT-κ-carrageenan-Fe_3O_4 nanocomposites, Environ. Pollut., 244 (2019) 723–732.

[71] N.H. Othman, N.H. Alias, M.Z. Shahruddin, N.F.A. Bakar, N.R.N. Him, W.J. Lau, Adsorption kinetics of methylene blue dyes onto magnetic graphene oxide, J. Environ. Chem. Eng., 6 (2018) 2803–2811.

[72] H.N. Bhatti, A. Jabeen, M. Iqbal, S. Noreen, Z. Naseem, Adsorptive behavior of rice bran-based composites for malachite green dye: isotherm, kinetic and thermodynamic studies, J. Mol. Liq., 237 (2017) 322–333.

[73] T. Maneerung, J. Liew, Y. Dai, S. Kawi, C. Chong, C.-H. Wang, Activated carbon derived from carbon residue from biomass gasification and its application for dye adsorption: kinetics, isotherms and thermodynamic studies, Bioresour. Technol., 200 (2016) 350–359.

[74] S.M. Pormazar, A. Dalvand, Adsorption of Direct Red 23 dye from aqueous solution by means of modified montmorillonite nanoclay as a superadsorbent: mechanism, kinetic and isotherm studies, Korean J. Chem. Eng., 37 (2020) 2192–2201.

[75] L. Mouni, L. Belkhiri, J.-C. Bollinger, A. Bouzaza, A. Assadi, A. Tirri, F. Dahmoune, K. Madani, H. Remini, Removal of Methylene Blue from aqueous solutions by adsorption on Kaolin: kinetic and equilibrium studies, Appl. Clay Sci., 153 (2018) 38–45.

[76] S. Kaushal, R. Badru, S. Kumar, H. Kaur, P. Singh, Efficient removal of cationic and anionic dyes from their binary mixtures by organic–inorganic hybrid material, J. Inorg. Organomet. Polym. Mater., 28 (2018) 968–977.

[77] O. Duman, E. Ayranci, Structural and ionization effects on the adsorption behaviors of some anilinic compounds from aqueous solution onto high-area carbon-cloth, J. Hazard. Mater., 120 (2005) 173–181.

[78] O. Duman, E. Ayranci, Adsorption characteristics of benzaldehyde, sulphanilic acid, and p-phenolsulfonate from water, acid, or base solutions onto activated carbon cloth, Sep. Sci. Technol., 41 (2006) 3673–3692.

[79] E. Hoseinzadeh, A.R. Rahmanie, G. Asgari, G. McKay, A.R. Dehghanian, Adsorption of Acid Black 1 by using activated carbon prepared from scrap tires: kinetic and equilibrium studies, J. Sci. Ind. Res., 71 (2012) 682–689.

[80] S. Nethaji, A. Sivasamy, Adsorptive removal of an acid dye by lignocellulosic waste biomass activated carbon: equilibrium and kinetic studies, Chemosphere, 82 (2011) 1367–1372.

[81] D. Sun, X. Zhang, Y. Wu, X. Liu, Adsorption of anionic dyes from aqueous solution on fly ash, J. Hazard. Mater., 181 (2010) 335–342.

[82] H. Najafi Saleh, M.H. Dehghani, R. Nabizadeh, A.H. Mahvi, K. Yaghmaeian, F. Hossein, M. Ghaderpoori, M. Yousefi, A. Mohammadi, Data on the Acid Black 1 dye adsorbtion from aqueous solutions by low-cost adsorbent-*Cerastoderma lamarcki* shell collected from the northern coast of Caspian Sea, Data Brief, 17 (2018) 774–780.

[83] E. Daneshvar, M. Kousha, M. Jokar, N. Koutahzadeh, E. Guibal, Acidic dye biosorption onto marine brown macroalgae: isotherms, kinetic and thermodynamic studies, Chem. Eng. J., 204–206 (2012) 225–234.

[84] M. Kousha, E. Daneshvar, H. Dopeikar, D. Taghavi, A. Bhatnagar, Box–Behnken design optimization of Acid Black 1 dye biosorption by different brown macroalgae, Chem. Eng. J., 179 (2012) 158–168.

[85] M. Mana, M.S. Ouali, L.C. de Menorval, J.J. Zajac, C. Charnay, Regeneration of spent bleaching earth by treatment with cethyltrimethylammonium bromide for application in elimination of acid dye, Chem. Eng. J., 174 (2011) 275–280.

[86] S. Dawood, T.K. Sen, C. Phan, Synthesis and characterization of slow pyrolysis pine cone bio-char in the removal of organic and inorganic pollutants from aqueous solution by adsorption: kinetic, equilibrium, mechanism and thermodynamic, Bioresour. Technol., 246 (2017) 76–81.

[87] A. Hassani, R.D.C. Soltani, S. Karaca, A. Khataee, Preparation of montmorillonite–alginate nanobiocomposite for adsorption of a textile dye in aqueous phase: isotherm, kinetic and experimental design approaches, J. Ind. Eng. Chem., 21 (2015) 1197–1207.

[88] G.K. Latinwo, A.O. Alade, S.E. Agarry, E.O. Dada, Process optimization and modeling the adsorption of polycyclic aromatic-congo red dye onto *Delonix regia* pod-derived activated carbon, Polycyclic Aromat. Compd., 41 (2019) 400–418.

[89] M.R. Fathi, A. Asfaram, A. Farhangi, Removal of Direct Red 23 from aqueous solution using corn stalks: isotherms, kinetics and thermodynamic studies, Spectrochim. Acta, Part A, 135 (2015) 364–372.

[90] J.J. Zhang, X.L. Yan, M.Q. Hu, X.Y. Hu, M. Zhou, Adsorption of Congo red from aqueous solution using ZnO-modified SiO_2 nanospheres with rough surfaces, J. Mol. Liq., 249 (2018) 772–778.

[91] K.-W. Jung, B.H. Choi, S.Y. Lee, K.-H. Ahn, Y.J. Lee, Green synthesis of aluminum-based metal organic framework for the removal of azo dye Acid Black 1 from aqueous media, J. Ind. Eng. Chem., 67 (2018) 316–325.

[92] A. Shehata, Removal of methylene blue dye from aqueous solutions by using treated animal bone as a cheap natural adsorbent, Int. J. Emerging Technol. Adv. Eng., 3 (2013) 507–513.

[93] D.A. Nimkar, S.K. Chavan, Removal of methylene blue dye (basic dye) from aqueous solution using sawdust as an adsorbent, Int. J. Eng. Res. Technol. (IJERT), 3 (2014).